Crystallization behaviour of Metglas 2826 MB ($Fe_{40}Ni_{38}Mo_4B_{18}$)

V S RAJA, KISHORE and S RANGANATHAN

Department of Metallurgy, Indian Institute of Science, Bangalore 560 012, India

Abstract. Differential scanning calorimetry, x-ray diffraction and transmission electron microscopy have been employed to determine the thermal stability and identify the crystalline phases on devitrification of Metglas 2826 MB. The glass crystallizes into γ-FeNiMo and fcc $(FeNi)_{23}B_6$ with activation energies of 270 and 375 kJ mol^{-1} respectively. The reactions are primary and polymorphic in nature. The influence of Mo towards crystallization of $Fe_{40}Ni_{40}B_{20}$ has been to enhance the formation of the fcc $(FeNi)_{23}B_6$ phase in preference to orthorhombic $(FeNi)_3B$ phase and to raise the thermal stability of the amorphous state.

Keywords. Crystallization; Kissinger plot; microstructure; metallic glass.

1. Introduction

The crystallization study of metallic glasses is of interest as it provides a means to understand the nucleation and growth processes in undercooled melts and determine the thermal stability of glasses (Ranganathan and Banerjee 1984; Ranganathan and Suryanarayana 1985). It also derives interest from the fact that a number of metastable phases can be synthesized through this route. We have studied the thermal and chemical stability of a series of Fe-Ni-B glasses and this study of Metglas 2826 MB forms a part of it (Raja 1986).

Metglas 2826 MB ($Fe_{40}Ni_{38}Mo_4B_{18}$), a product of Allied Corporation (USA), has drawn considerable interest towards understanding its thermal stability (Antonione *et al* 1978, 1981; Azam *et al* 1979; Mizgalski *et al* 1981; Nicolai *et al* 1981; Battezzati *et al* 1982; Cumbrera *et al* 1982a, b; Menon and Suryanarayana 1985).

Employing non-isothermal DSC measurements, Antonione *et al* (1978) reported two-stage crystallization processes at 703 K and 777 K having activation energies of 296 and 334 kJ mol^{-1} respectively for the first and second crystallization reactions. However, Majumdar and Nigam (1980) and Cumbrera *et al* (1982b) observed a three-stage crystallization of the glass. DTA measurement by Majumdar and Nigam (1980) showed crystallization peaks at 728, 810 and 863 K. Cumbrera *et al* (1982b) determined activation energies both from Kissinger (288 and 355 kJ mol^{-1}) and isothermal (288 and 451 kJ mol^{-1}) methods using DTA, DSC and resistivity measurements for the first two crystallization processes. It may be noted that the activation energy deduced from the isothermal method for the second crystallization differs significantly from that obtained by the Kissinger method.

Mizgalski *et al* (1981) studied the sequence of crystallization using XRD. Their studies indicate that the first phase to crystallize from the glass is the fcc $(FeNi)_{23}B_6$, followed by the formation of a γ-FeNiMo solid solution. At high temperature $(FeNi)_3B$-bct phase was produced. An orthorhombic $(FeNi)_3B$ phase was found in samples annealed in a vacuum of 2×10^{-5} torr. Interestingly, Battezzati *et al* (1982) reported the presence of an orthorhombic Ni_3B phase in Metglas 2826 MB annealed at about 1000 K even without subjecting the glass to vacuum.

The observations by Nicolai *et al* (1981) are interesting in this context. They interpreted their DSC and Guinier high temperature camera experiments to indicate several stages of reaction. Phase separation was observed as a precrystallization process. The first crystal to form was γ-FeNiMo solid solution. This was followed by the formation of fcc $(FeNi)_{23}B_6$ phase by a peritectoid reaction of the γ-phase with the remaining glass of composition $(FeNiMo)_{75}B_{25}$. Eventhough reactions other than primary, eutectic and polymorphic have been speculated upon in the literature (Ranganathan and Banerjee 1984), this is the first time that a peritectoid reaction has been claimed to occur.

In a limited but direct microstructural study by TEM, Cumbrera *et al* (1982a) observed the appearance of γ-FeNiMo followed by fcc $(FeNi)_{23}B_6$. Subsequent heating to high temperature led to a stable phase whose structure was not determined.

Menon and Suryanarayana (1985) have recently brought out the difference between the crystallization behaviour of the vapour deposited and liquid quenched Metglas 2826 MB using TEM. The vapour-deposited glass leads to a fcc solid solution, which is different from the γ-FeNiMo phase formed during annealing. Furthermore, it has been pointed out that the vapour-deposited glass yields a simple cubic phase instead of the fcc boride phase crystallizing in melt quenched glass.

As seen above, the review of the literature on Metglas 2826 MB shows that, in spite of extensive work, diverse views exist among several investigators regarding the crystallization process. The present study is undertaken to address the following points over which differences exist in the literature: (a) the number of stages of crystallization (two, three or more); (b) the order of appearance of the crystalline phase (γ-FeNiMo and $(FeNiMo)_{23}B_6$)); (c) the nature of the second stage of crystallization (Polymorphic or peritectoid); (d) the possibility of phase separation preceding crystallization.

2. Experimental procedure

Metglas 2826 MB obtained from Allied Corporation, USA was in the form of ribbons of width 15 mm and thickness 35 μm. The nominal composition in atomic percentage was $Fe_{40}Ni_{38}Mo_4B_{18}$. A Perkin Elmer DSC 2C was used to determine the crystallization temperatures. In order to get a true value of crystallization temperature free from the thermal gradients of the instrument, the method of Meisel and Cote (1983) was adopted. The phases present in the annealed samples were analysed using a Philips 1140 x-ray diffractometer (XRD) with CoKα radiation of wavelength 0·17902 nm. The microstructures were observed under a Philips 301 electron microscope operating at 100 kV. Thin samples for transmission electron microscopy were obtained using a Tenupol twin jet electropolisher controlled by Struers variable potential stabilizer. A good polishing was obtained with an electrolyte of 20% methanol and 80% sulphuric acid maintained at $-10°C$ and with an operating DC volt of 10.

3. Results and discussion

3.1 *Differential scanning calorimetry*

The glass subjected to constant heating rates in DSC for 10, 20, 40 and 80 K min^{-1}

between 320 and 1000 K exhibited two exothermic peaks (the typical DSC trace for the heating rate 10 K min^{-1} is shown in figure 1). This agrees with the results of Antonione *et al* (1978) but shows disagreement with other results which reported three (Majumdar and Nigam 1980; Cumbrera *et al* 1982b) and four (Nicolai *et al* 1981) exothermic peaks. However, it can be noted that the peak temperatures for the first and second peaks reported by these investigators agree well with the present values. Additional support for the two-stage crystallization is found in the fact that for a variety of (FeNiMo)B glasses, Antonione *et al* (1980) have found only two stages. The nature of crystalline phases formed under these peaks will be discussed in §§ 3·2 and 3·3 using XRD and TEM.

The peak shift with heating rates has been exploited to determine the activation energy for crystallization employing Kissinger's (1957) equation

$$\ln \beta/T_p^2 = - E_c/RT_p + C, \tag{1}$$

where β, T_p, E_c and C respectively represent the heating rate, peak temperature, apparent activation energy and a constant. The Kissinger plots of $\ln \beta/T_p^2$ vs $1/T_p$ are shown in figure 2. The E_c values turn out to be 270 and 375 kJ mol^{-1} respectively for the first and second crystallization processes. The values compared with earlier results reported in the literature are given in table 1. In a majority of the cases the present values agree with the earlier reported results. However, two differences can be noticed: (i) Nicolai *et al* (1981) reported higher values of activation energies for both the transitions and   (ii) Cumbrera *et al* (1982b) estimated a higher value from the isothermal kinetics for the second crystallization reaction. It should be remarked that the activation energy determined by Cumbrera *et al* (1982b) using non-isothermal kinetics is in close agreement with the present results. It is also relevant to note that though the apparent activation energies obtained through DSC and microscopy techniques have been widely employed to compare the thermal stabilities of amorphous alloys, Berkenpas *et al* (1986) expressed reservation towards meaningful interpretation of the crystallization mechanisms.

3.2   *X-ray diffraction*

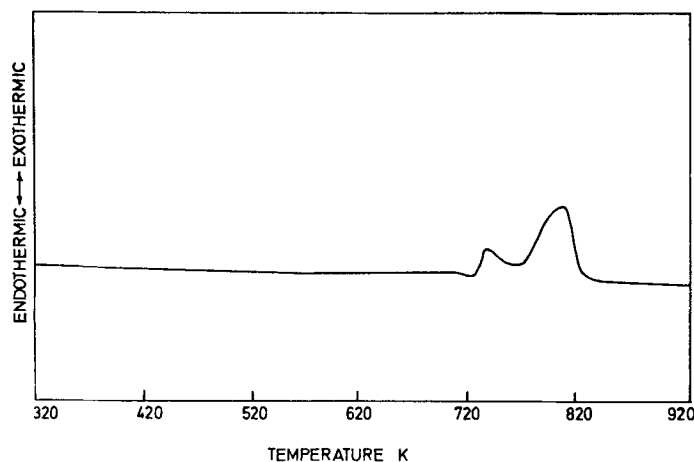The phases crystallizing out during the first and second exothermic reactions are

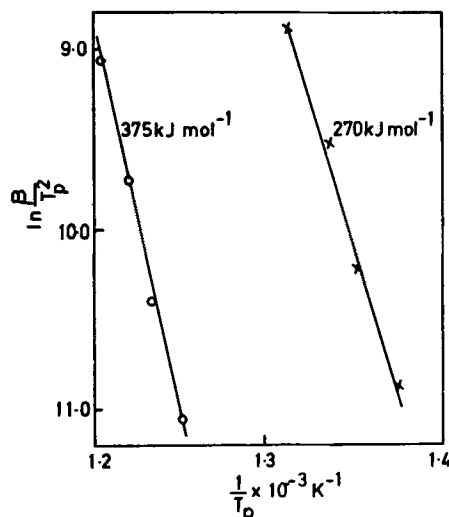**Figure 1.**   DSC trace of Metglas 2826 MB for the heating rate of 10 K min^{-1}.

Figure 2. Kissinger plots for the first and second crystallization process.

Table 1. Comparison of activation energies for the crystallization of Metglas 2826 MB.

MS I $kJ\,mol^{-1}$	MS II $kJ\,mol^{-1}$	Method of determination	References
270	375	Kissinger	Present work
296	334	Ozawa	Antonione *et al* (1978)
*403	415	Kissinger	Nicolai *et al* (1981)
288	355	Kissinger	Cumbrera *et al* (1982b)
288	451	Isothermal kinetics	—''—

*The values correspond to the second and third peaks, where γ-FeNiMo and fcc $(FeNi)_{23}B_6$ are reported, whereas these phases have been found to crystallize under first and second peaks of the DSC curve according to other investigators.

identified by heating the glass till the end of the peaks in DSC, cooling it back to room temperature with a cooling rate of $320\ K\ min^{-1}$ and subsequently analysing it in XRD. Phase transition in the crystallized glass, if any, at high temperature is identified by heating the glass in DSC upto 1000 K. These XRD results are summarized in figure 3. The XRD of the amorphous alloy is extremely broad (figure 3a). The k value ($=4\pi \sin\theta/\lambda$) determined from the half width of the half maxima turns out to be $31\cdot1\ nm^{-1}$. The broad peak becomes sharper in the case of the sample annealed till the end of the first peak of the DSC trace (figure 3b). The peak corresponds to (111) of γ-FeNiMo phase with the lattice parameter 0·358 nm. The other peaks are not visible owing to the low volume of γ-FeNiMo present in the sample. Distinct peaks appear in the x-ray diffractogram (figure 3c) of the glass annealed till the end of the second exothermic peak which are indexed satisfactorily on the basis of fcc $(FeNi)_{23}B_6$ phase with $a = 1\cdot061$ nm. It should be noted that the peak corresponding to (111) of γ-FeNiMo phase merges with that of (333) of $(FeNi)_{23}B_6$ in this case. The glass annealed upto 1000 K shows significant volume of γ-FeNiMo phase which might have transformed from fcc $(FeNi)_{23}B_6$ boride phase.

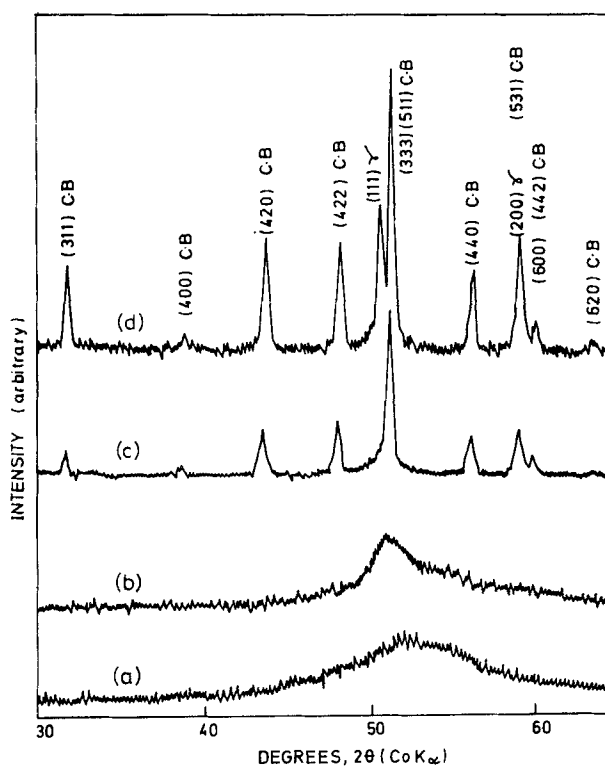**Figure 3.** X-ray diffractograms showing the sequence of crystallization: **(a)** amorphous **(b)** heated upto 760 K **(c)** heated upto 860 K and **(d)** heated upto 1000 K. (C.B. refers to cubic boride).

3.3 *Transmission electron microscopy*

The microstructure and the corresponding selected area diffraction (SAD) pattern of the as-received amorphous alloy is shown are figure 4. The glass possesses a mottled structure and the unusually broad halo rings (especially the first ring) complement the XRD of the amorphous alloy shown in figure 3a. This may be attributed to phase separation. Such an instance of phase separation in an as-quenched glass has earlier been reported in Fe-B alloys by Walter and Bartram (1978). However, the mottled structure may be due to the preferential dissolution during electropolishing. Cumbrera *et al* (1982a) have indeed explained their microstructure on this basis. As has been observed by Walter and Bartram (1978), two sets of haloes are not detected in this glass. Further, there was no evidence for two glass transition temperatures. Thus incipient phase separation remains only a possibility, without adequate evidence. It has to be pointed out that among the many investigators, only Nicolai *et al* (1981) have postulated phase separation.

The development of microstructure has been studied for the isothermal annealing at 773 K using TEM. Figure 5 shows the microstructure, SAD pattern and dark field image (corresponding to the second ring of the pattern) for the glass annealed for 15 min at 773 K. The SAD pattern can be indexed satisfactorily for γ-FeNiMo phase with $a = 0.358$ nm and the dark field image reveals almost spherical crystals
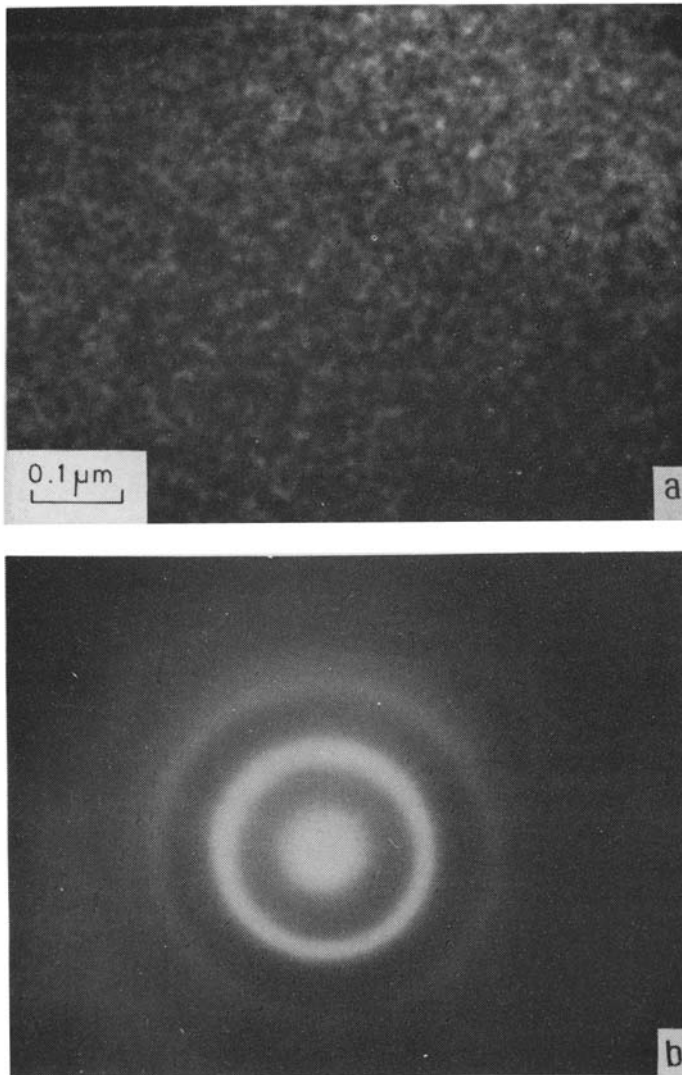
Figure 4. **a.** Bright field image. **b.** SAD pattern of the amorphous alloy. Note the mottled structure in the micrograph.

embedded in the matrix. The fcc $(FeNi)_{23}B_6$ crystals start emerging from the specimen annealed for 30 min and their number and size increase with time. A complete crystallization is noticed in the alloy annealed for 120 min. Figure 6 shows the microstructure of the partially crystallized glass (773 K, 45 min). The crystals possess a faceted morphology. Figure 7 shows the bright field image, SAD pattern and the dark field image of the fully crystallized (773 K, 120 min) glass. On close examination some of the fcc $(FeNi)_{23}B_6$ crystals exhibit twins/faults in them.

Figure 5. **a.** Bright field image. **b.** Corresponding SAD pattern. **c.** Dark field image of the glass annealed at 773 K for 15 min. The continuous rings belong to γ-FeNiMo phase.
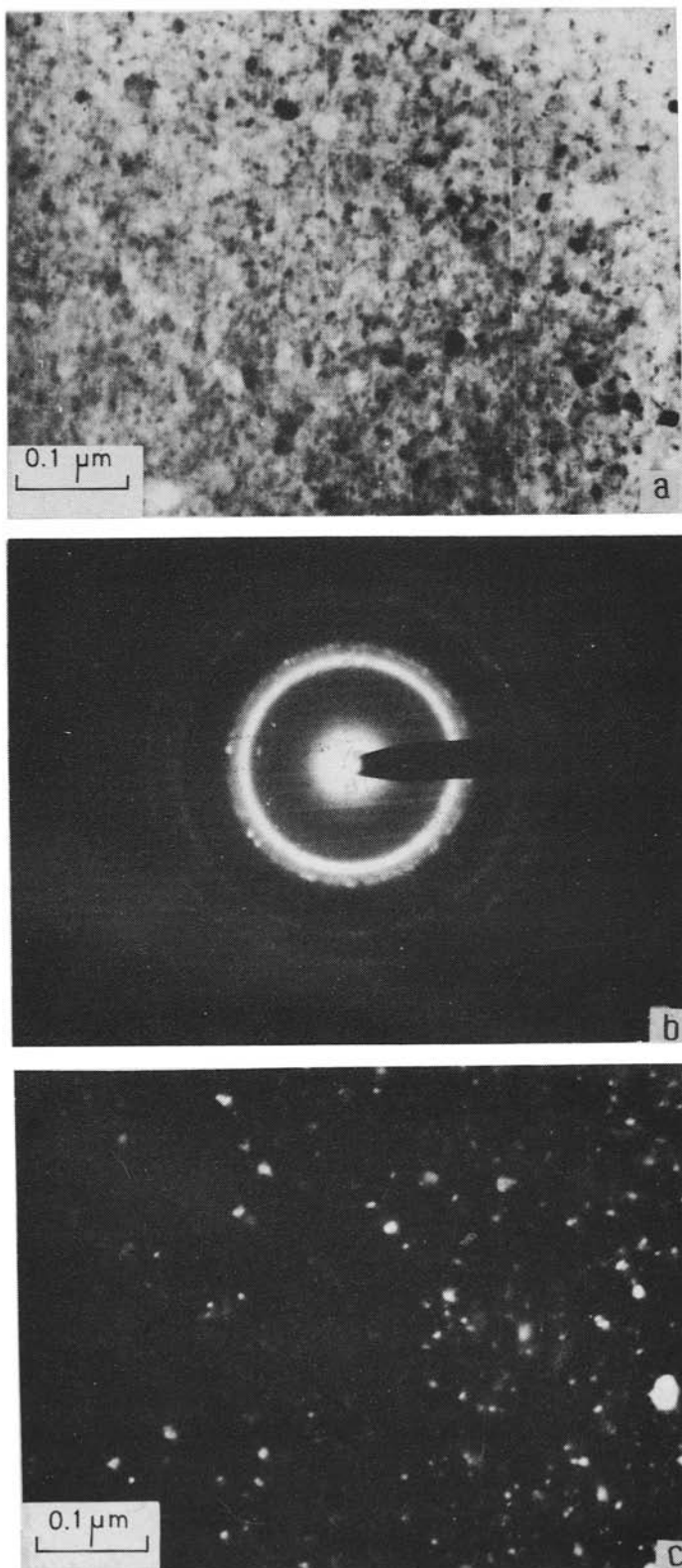
Figure 5.

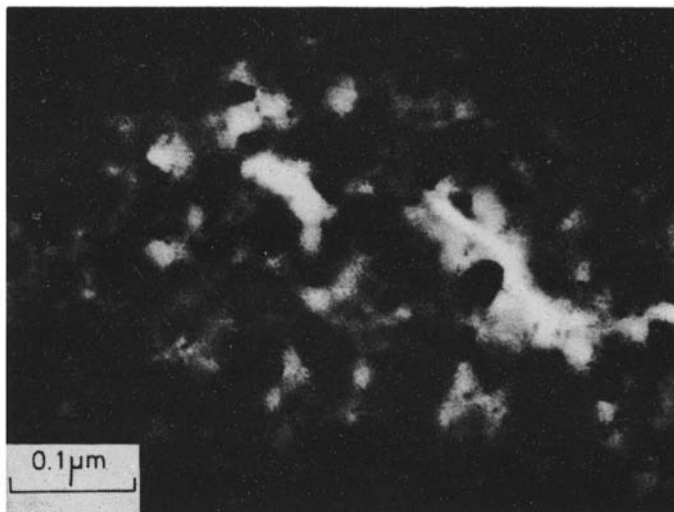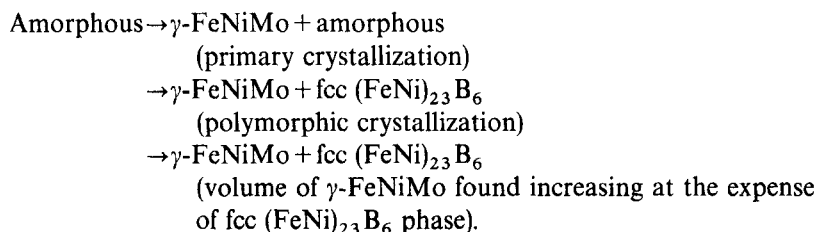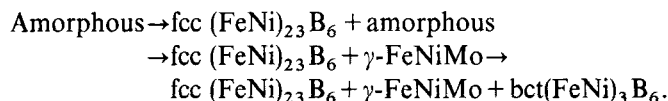**Figure 6.** Well grown fcc $(FeNi)_{23}B_6$ crystals in the glass annealed at 773 K for 45 min.

Interestingly, fcc $(FeNi)_{23}B_6$ crystals grow with the same morphology at low temperature (723 K, 60 min) as illustrated by the micrograph of figure 8.

The following scheme of sequence of phase transition in Metglas 2826 MB can be derived from the DSC, XRD and TEM studies.

$$\text{Amorphous} \rightarrow \gamma\text{-FeNiMo} + \text{amorphous}$$
$$\text{(primary crystallization)}$$
$$\rightarrow \gamma\text{-FeNiMo} + \text{fcc } (FeNi)_{23}B_6$$
$$\text{(polymorphic crystallization)}$$
$$\rightarrow \gamma\text{-FeNiMo} + \text{fcc } (FeNi)_{23}B_6$$
$$\text{(volume of } \gamma\text{-FeNiMo found increasing at the expense}$$
$$\text{of fcc } (FeNi)_{23}B_6 \text{ phase).}$$

It can be noted that fcc $(FeNi)_{23}B_6$ phase is metastable (Herold and Koster 1978) and hence can transform into γ-FeNiMo phase. The sequence of formation of γ-FeNiMo followed by fcc $(FeNi)_{23}B_6$ is in accordance with the observations of Nicolai *et al* (1981) and Cumbrera *et al* (1982a). However, Mizgalski *et al* (1981) reported a different sequence as follows

$$\text{Amorphous} \rightarrow \text{fcc } (FeNi)_{23}B_6 + \text{amorphous}$$
$$\rightarrow \text{fcc } (FeNi)_{23}B_6 + \gamma\text{-FeNiMo} \rightarrow$$
$$\text{fcc } (FeNi)_{23}B_6 + \gamma\text{-FeNiMo} + \text{bct}(FeNi)_3B_6.$$

Comparing the above sequences of crystallization with the present one indicates that they have not identified the initial formation of γ-FeNiMo from the glass but have reported the phase transition from fcc $(FeNi)_{23}B_6$ to γ-(FeNiMo) phase in the crystallized glass.

Figure 7. **a.** Microstructure. **b.** SAD pattern. **c.** Dark field image of the fully crystallized glass (annealing treatment 773 K, 120 min).
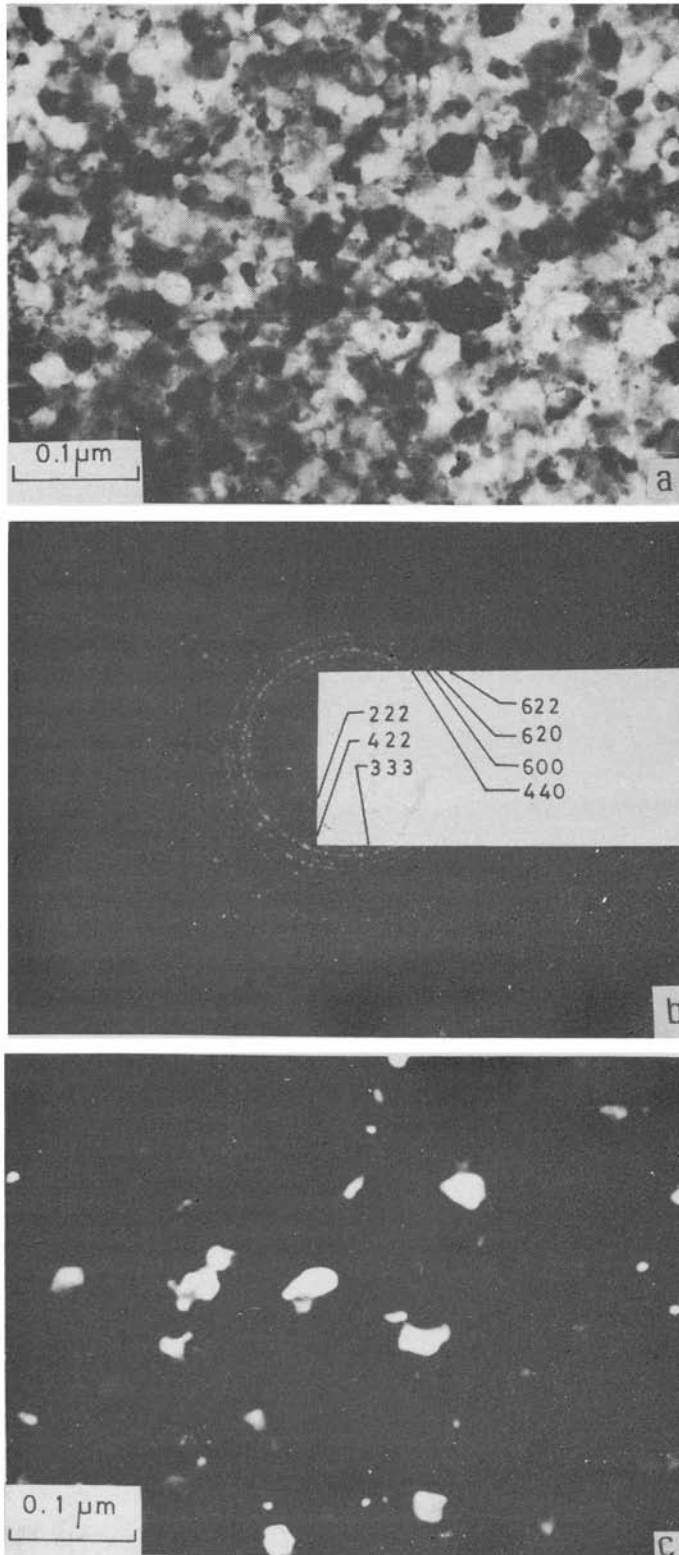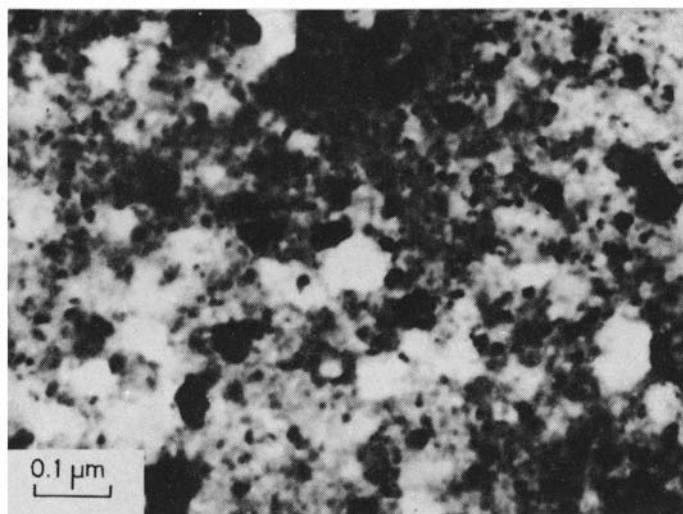
Figure 7.

Figure 8. Microstructure of Metglas 2826 MB annealed for 60 min at 723 K.

In addition to the γ and boride phases, Mizgalski *et al* (1981) noticed the formation of bct $(FeNi)_3 B$ above 950 K and Battezzati *et al* (1982) identified an orthorhombic $Ni_3 B$ phase at about 1000 K. However, the present study does not indicate any of the two phases either in x-ray or in TEM studies. Interestingly, neither Nicolai *et al* (1981) nor Menon and Suryanarayana (1985) found the presence of bct $(FeNi)_3 B$ and orthorhombic $Ni_3 B$ phases.

The influence of Mo towards the crystallization of FeNiB glasses is more striking when the crystallization characteristics of $Fe_{40} Ni_{40} B_{20}$ glass is compared with that of Metglas 2826 MB. Raja (1986) has reported that the glass $Fe_{40} Ni_{40} B_{20}$ crystallizes into four types of crystals. The first two of them are eutectic mixtures of γ-FeNi + orthorhombic $(FeNi)_3 B$ and γ-FeNi + fcc $(FeNi)_{23} B_6$ and the third and the fourth are a single phase γ-FeNi solid solution and an unknown Fe-rich phase. Although we find fcc $(FeNi)_{23} B_6$ phase in $Fe_{40} Ni_{40} B_{20}$, its volume fraction is $< 5\%$ (could not be identified by x-ray diffraction and was possible to detect only in TEM). Hence it is very obvious that Mo enhances the formation of a fcc $(FeNi)_{23} B_6$ phase in preference to the orthorhombic $(FeNi)_3 B$ phase. Further, in the presence of Mo, crystallization takes place by simple two-stage processes in contrast to the complex single-stage crystallization in Mo-free $Fe_{40} Ni_{40} B_{20}$ glass simultaneously imparting a thermal stability to the glass.

4. Conclusions

(i) XRD and TEM studies have indicated that the glass crystallizes in two stages into γ-FeNiMo followed by fcc $(FeNi)_{23} B_6$. The same sequence is reported by Nicolai *et al* (1981) and Cumbrera *et al* (1982a). Additional stages observed by other investigators are due to the transformation of the crystalline state to more stable states.

(ii) The γ-FeNiMo phase forms by the primary mode as noted by Nicolai *et al*

(1981), while the fcc $(FeNi)_{23}B_6$ forms by a polymorphic mode and not by the peritectoid mode as suggested by Nicolai *et al* (1981).

(iii) The activation energies for the devitrification of the glass into γ-FeNiMo and fcc $(FeNi)_{23}B_6$ phases respectively turn out to be 270 and 375 kJ mol^{-1} from the Kissinger plots.

(iv) Though the appearance of the pseudograin structure and the broad XRD peak can be attributed to the incipient phase separation of the glass during melt quenching itself, it is felt that the evidence for phase separation is not strong.

(v) It is confirmed that the addition of molybdenum enhances the thermal stability of (FeNiB) glasses and leads to the formation of fcc $(FeNi)_{23}B_6$ in preference to orthorhombic $(FeNi)_3B$.

Acknowledgements

References

Antonione C, Battezzati L, Lucci A, Riontino G and Venturello G 1978 *Scr. Metall.* **12** 1011

Antonione C, Battezzati L, Lucci A, Riontino G, Tabasso M C and Venturello G 1980 *J. Phys. (Paris)* **C41** 131

Antonione C, Battezzati L, Lucci A, Riontino G and Venturello G 1981 *La Metall.* **73** 118

Azam N, Lenaour L, Rivera C, Grosjean P, Sacovy P and Delaplace J 1979 *J. Nucl. Mater.* **83** 298

Battezzati L, Antonione C and Cossolo A 1982 *Z. Metallkd.* **73** 185

Berkenpas M B, Barnard J A, Ramanujam R V and Aaronson H I 1986 *Scr. Metall.* **20** 323

Cumbrera F L, Millan M, Conde A, Marquez R and Vigier P 1982a *J. Mater. Sci.* **17** 861

Cumbrera F L, Miranda H, Conde A, Marquez R and Vigier P 1982b *J. Mater. Sci.* **17** 2677

Herold U and Koster U 1978 *Z. Metallkd.* **69** 326

Kissinger H E 1957 *Anal. Chem.* **29** 1702

Majumdar A K and Nigam A K 1980 *J. Appl. Phys.* **51** 4218

Meisel L V and Cote P J 1983 *Acta Metall.* **31** 1053

Menon J and Suryanarayana C 1985 *Z. Metallkd.* **76** 802

Mizgalski K P, Inal O T, Yost P G and Karnowsky M M 1981 *J. Mater. Sci.* **16** 3357

Nicolai H P, Kopmann G and Trommeyer G 1981 *Z. Metallkd.* **72** 558

Raja V S 1986 *Thermal and chemical stabilities of three Fe-Ni-B metallic glasses*, Ph.D. Thesis, Indian Institute of Science, Bangalore

Ranganathan S and Banerjee S 1984 *Metallic glasses production, properties and application* (ed.) T R Anantharaman (Switzerland: Trans-Tech Publications) p 147

Ranganathan S and Suryanarayana C 1985 *Mater. Sci. Forum* **4** 173

Walter J L and Bartram S F 1978 *Rapidly quenched metals* (ed.) B Cantor (London: The Metal Society) Vol. 1, p 307